RECOMMENDATION ITU-R P.843-1

COMMUNICATION BY METEOR-BURST PROPAGATION

(Question ITU-R 221/3)

(1992-1997)

The ITU Radiocommunication Assembly,

considering

a)   that scattering from ionization caused by meteor trails can provide a convenient means of communication at HF and VHF;

b)   that two-way telecommunication circuits are in operation with frequencies between 30 and 100 MHz over ranges up to 1 800 km;

c)   that communication relies on bursts of propagation during the occurrence of meteor trails and can support data rates up to 100 Bd when averaged over approximately one hour,

recommends

that the following information should be used in the design and planning of meteor-burst communications systems.

1   Temporal variations in meteor flux

At certain times of the year, meteors occur in the form of showers and may be prolific over durations of a few hours. There is, however, a general background of meteors incident upon the Earth from all directions and it is appropriate to consider only these sporadic meteors for communication-planning purposes.

For sporadic meteors at mid-latitudes there is a roughly sinusoidal diurnal variation of incidence with a maximum at 0600 h and a minimum at 1800 h local time. The ratio of maximum to minimum averages about four. In the Northern Hemisphere there is a seasonal variation of similar magnitude with a minimum in February and maximum in July. Considerable day-to-day variability exists in the incidence of both sporadic and shower meteors.

The annual average flux of meteors incident per unit area and producing electron-line densities q exceeding a threshold q_0 per metre, $I\,(q > q_0)$ is given as:

$$I(q \, > \, q_0) \; = \; \frac{160}{q_0} \qquad \text{m}^{-2}\,\text{s}^{-1} \qquad\qquad (1)$$

By combining this overall meteor rate with a representative sinusoidal diurnal variation and the seasonal factor, M, from Fig. 1 the average temporal changes in meteor flux can be estimated:

$$\frac{160}{q_0} \; M \left[\, 1 \; + \; 0.6 \left(\sin \frac{\pi T}{12} \right) \right] \qquad \text{m}^{-2}\,\text{s}^{-1} \qquad\qquad (2)$$

where:

T: local time (h).

For planning purposes it may only be necessary to consider the worst combination of month and local time.

2   Spatial variation in meteor flux

Meteors occur in all parts of the world at all hours but statistical information is incomplete on their geographical distribution and trail directions.

FIGURE 1

**Month-to-month variation in sporadic meteor flux rate
relative to the average value**
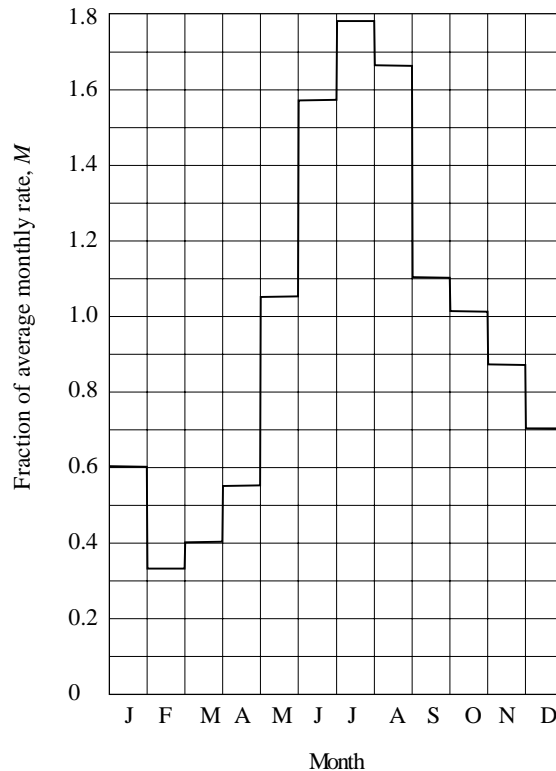
0843-01

Until such times as spatial variations are quantified it is recommended that flux estimates based on the method given in § 1 are used at all latitudes.

3   Underdense and overdense trails

The ionized trails caused by meteors are classified as underdense or overdense according to the intensity of the ionization. The division between the two cases occurs for line densities of approximately 2×10^{14} electrons per metre. The amplitude of signals scattered from underdense trails may be calculated by summing the scattered field arising from each individual electron. Overdense trails are those for which the coupling between electrons cannot be ignored, in which case, the reflecting properties are calculated as if the trail were a long metallic cylinder. At frequencies used in practice the echoes from underdense trails show an abrupt start followed by an exponential decay, whereas those from overdense trails have more rounded envelopes and are of longer duration. The relative proportions of underdense and overdense echoes will depend on the system sensitivity.

The relation between number of trails and peak amplitude, A, can be approximated by:

$$\text{Number of trails} \propto (A)^{-\psi}$$

where ψ varies from 1.0 at low signal levels to greater than 2.0 at larger signal levels where the majority of trails are overdense. For many links, the index ψ is of the order of 1.1 to 1.4.

Results in the systems used so far indicate that echoes are predominantly from underdense trails. On this basis it is recommended that planning for a typical system should proceed on the basis that all meteor trails are of the underdense type.

4 Effective length and radius of meteor trails

4.1 Effective length

The ray geometry for a meteor-burst propagation path is shown in Fig. 2 between transmitter T and receiver R. P represents the tangent point and P′ a point further along the trail such that $(R'_1 + R'_2)$ exceeds $(R_1 + R_2)$ by half a wavelength. Thus PP′ (of length L) lies within the principal Fresnel zone and the total length of the trail within this zone is $2L$. Provided R_1 and R_2 are much greater than L, it follows that for practical cases:

$$L = \left[\frac{\lambda\, R_1\, R_2}{(R_1 + R_2)\,(1 - \sin^2 \varphi \cos^2 \beta)} \right]^{1/2}$$
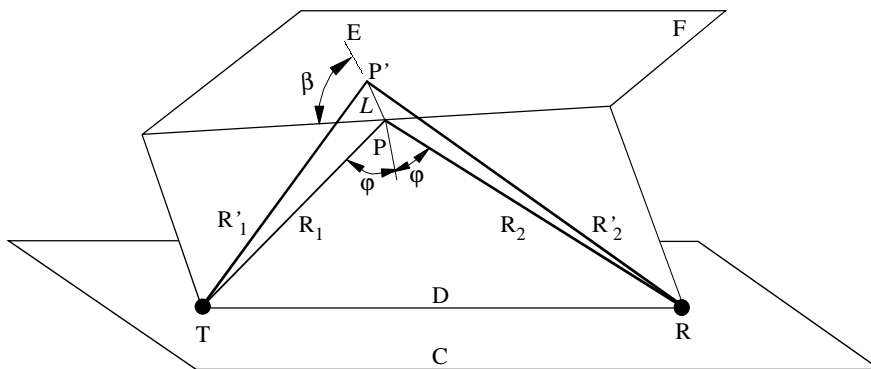(3)

where:

φ : angle of incidence

β : angle between the trail axis and the plane of propagation

λ : wavelength.

FIGURE 2

Ray geometry for a meteor-burst propagation path

C: Earth's surface
D: plane of propagation
E: trail
F: tangent plane
β: angle between the trail axis and the plane of propagation
T: transmitter
R: receiver

0843-02

4.2 Trail radius

In order to evaluate the scattering cross section of the trail it is usual to assume that ambipolar diffusion causes the radial density of electrons to have a Gaussian distribution and that the volume density is reduced while the line density remains constant.

The ionization trail immediately behind a meteor is formed near-instantaneously with a finite width. This is called the initial trail radius, r_0. An empirical relationship between r_0, and the meteor height is:

$$\log r_0 = 0.035\, h - 3.45$$
(4)

where:

h : trail height (km)

r_0 : initial trail radius (m).

5   Received power and basic transmission loss

5.1   Received power

Since any practical meteor-burst communication system will rely mainly on underdense trails, the overdense formulae are of less importance. Satisfactory performance estimates can be made using formulae for the underdense case with assumed values of q in the range 10^{13} to 10^{14} electrons per metre according to the prevailing system parameters.

The received power $p_R(t)$ after scattering from underdense trails at frequencies used in practice is as follows:

$$p_R(t) = \frac{p_T \, g_T \, g_R \, \lambda^2 \, \sigma \, a_1 \, a_2(t) \, a_2(t_0) \, a_3}{64\pi^3 \, R_1^2 \, R_2^2} \tag{5}$$

where:

λ :   wavelength (m)

σ :   echoing area of the trail (m^2)

a_1 :   loss factor due to finite initial trail radius

$a_2(t)$:   loss factor due to trail diffusion

a_3 :   loss factor due to ionospheric absorption

t :   time in seconds measured from the instant of complete formation of the first Fresnel zone

t_0 :   half the time taken for the meteor to traverse the first Fresnel zone

p_T :   transmitter power (W)

$p_R(t)$:   power available from the receiving antenna (W)

g_T :   transmit antenna gain relative to an isotropic antenna in free space

g_R :   receive antenna gain relative to an isotropic antenna in free space

(Lossless transmitting and receiving antennas are assumed)

R_1, R_2 : distances (m) see Fig. 2.

The echoing area σ is given as:

$$\sigma = 4 \pi \, r_e^2 \, q^2 \, L^2 \, \sin^2 \alpha \tag{6}$$

where:

r_e : effective radius of the electron $= 2.8 \times 10^{-15}$ m

α : angle between the incident electric vector at the trail and the direction of the receiver from that point.

Since L^2 is directly proportional to λ, the echoing area, σ, is also proportional to λ and hence the received power for underdense trails varies as λ^3. Horizontal polarization normally is used at both terminals. The $\sin^2 \alpha$ term in equation (6) is then nearly unity for trails at the two hot spots.

The loss factor a_1 is given by:

$$a_1 = \exp \left[-\frac{8 \pi^2 r_0^2}{\lambda^2 \sec^2 \varphi} \right] \tag{7}$$

It represents losses arising from interference between the re-radiation from the electrons wherever the thickness of the trail at formation is comparable with the wavelength.

The factor $a_2(t)$ allows for the increase in radius of the trail by ambipolar diffusion. It may be expressed as:

$$a_2(t) = \exp\left[-\frac{32\,\pi^2\,D\,t}{\lambda^2\,\sec^2\,\varphi}\right] \tag{8}$$

where D is the ambipolar diffusion constant in $m^2\,s^{-1}$ given by:

$$\log D = 0.067\,h - 5.6 \tag{9}$$

The increase in radius due to ambipolar diffusion can be appreciable even for as short a period as is required for the formation of the trail. The overall effect with regard to the reflected power is equal to that which would arise if the whole trail within the first Fresnel zone had expanded to the same extent as at its mid-point. Since this portion of trail is of length $2L$ the mid-point radius is that arising after a time lapse of L/V (s) where V is the velocity of the meteor in ms^{-1} Calling the time lapse t_0 gives, for trails near the path mid-point ($R_1 \approx R_2 = R$):

– For trails at right angles to the plane of propagation ($\beta = 90°$):

$$t_0 \simeq \left(\frac{\lambda R}{2\,V^2}\right)^{\frac{1}{2}} \tag{10}$$

– For trails in the plane of propagation ($\beta = 0°$):

$$t_0 \simeq \left(\frac{\lambda R}{2\,V^2}\right)^{1/2} \cdot \sec\,\varphi \tag{11}$$

Substituting t_0 from equation (10) into equation (8) gives for the $\beta = 90°$ case:

$$a_2(t_0) = \exp\left[-\frac{32\,\pi^2}{\lambda^{3/2}}\left(\frac{D}{V}\right)\left(\frac{R}{2}\right)^{1/2}\frac{1}{\sec^2\,\varphi}\right] \tag{12}$$

For $\beta = 0°$ the exponent in this expression is $\sec\,\varphi$ times greater.

The ratio of the ambipolar diffusion constant D to the velocity of the meteor V (required in the evaluation of received power) can be approximated by:

$$D/V = \left[0.0015\,h + 0.035 + 0.0013\,(h - 90)^2\right]\,10^{-3} \tag{13}$$

$a_2(t)$ is the only time-dependent term and gives the decay time of the reflected signal power. Defining a time constant T_{un} for the received power to decay by a factor e^2 (i.e. 8.7 dB) leads to:

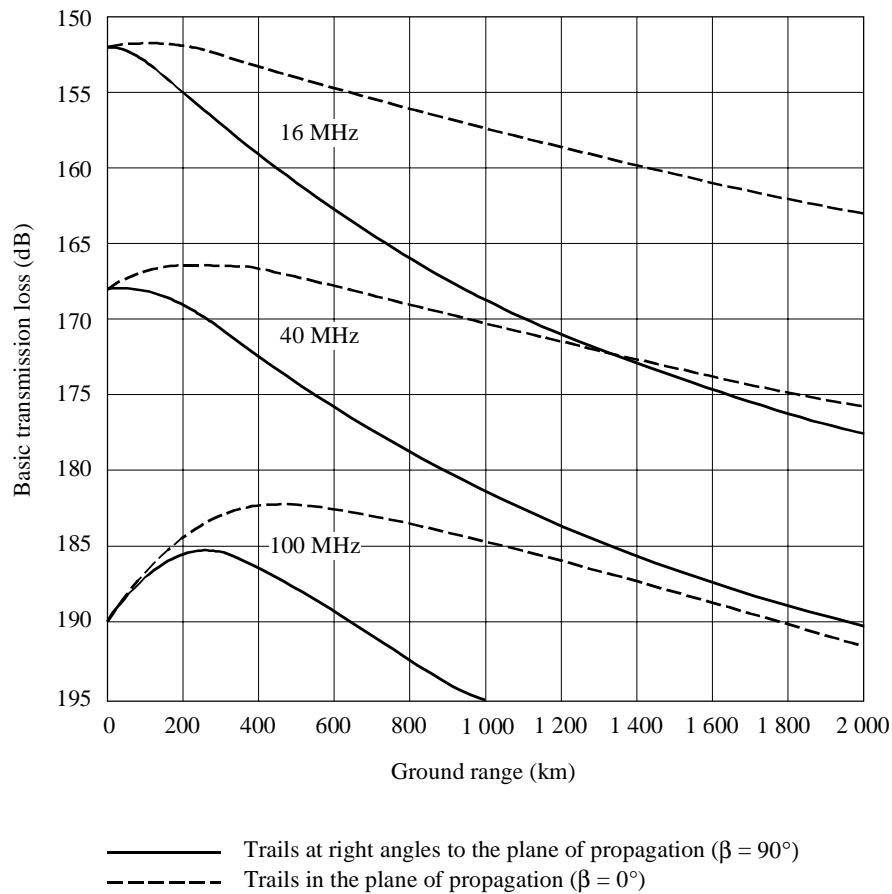$$T_{un} = \frac{\lambda^2\,\sec^2\,\varphi}{16\,\pi^2\,D} \tag{14}$$

With reflection at grazing incidence $\sec^2\,\varphi$ will be large and hence so is the echo-time constant. The echo-time constant is also increased by the use of lower frequencies.

5.2   Basic transmission loss

Basic transmission loss curves derived from equation (5) with $q = 10^{14}$ electrons per metre are given in Fig. 3. As the angle β can take any value between $0°$ and $90°$ only these two extreme cases are shown. The advantage of lower propagation loss at the lower frequencies is clearly seen. Average meteor heights given from equation (15) have been used in deriving the curves. It should be noted that the prediction of system performance depends critically on the heights assumed.

FIGURE 3

**Basic transmission loss for underdense trails given by equation (5)
with $q = 10^{14}$ electrons/m and horizontal polarization**

Trails at right angles to the plane of propagation ($\beta = 90°$)
- - - - - - Trails in the plane of propagation ($\beta = 0°$)

0843-03

6   The underdense echo ceiling and average trail height

Both the initial trail radius, r_0, and the ambipolar diffusion constant, D, increase with altitude. Consequently, the loss factors a_1 and $a_2(t_0)$ combine to reduce the number of underdense meteors occurring near the top of the meteor region which are useful for communication purposes. This effect is usually referred to as the underdense echo ceiling. Similar constraints have been observed to exist in the monostatic case. Figure 4 shows the measured height distribution of underdense echoes using various radar frequencies.

It can be seen that the lowest altitude at which underdense echoes occur is 85 km, and that the altitude distribution is approximately Gaussian at any frequency.

The average trail height h (km) at frequency f (MHz) is:

$$h = -17 \log f + 124 \tag{15}$$

The average trail height is a function of other system parameters in addition to frequency. However equation (15) is a good approximation.

FIGURE 4

**Height distribution of underdense meteors providing echoes
at frequencies of 18, 36 and 70 MHz**
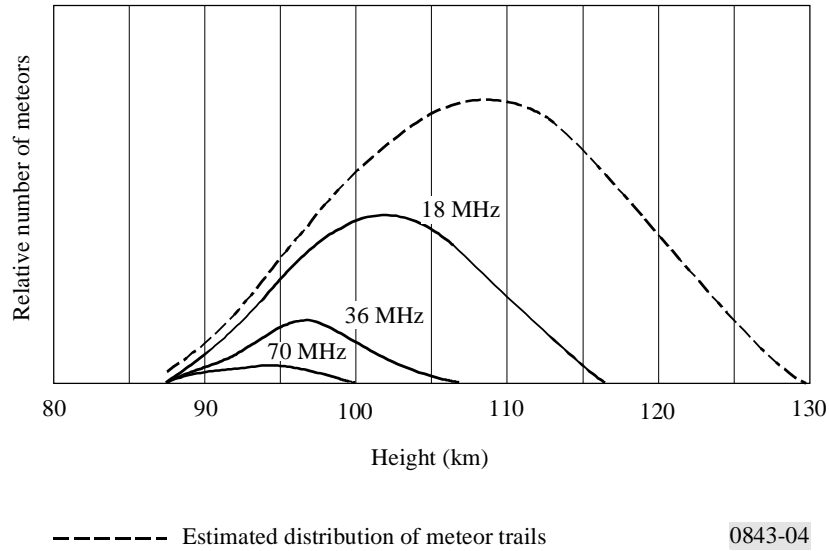
- - - - - - Estimated distribution of meteor trails　　　　　　0843-04

7　　Positions of regions of optimum scatter

The scattering properties of straight meteor ionization trails are strongly aspect sensitive. To be effective, it is necessary for the trails approximately to satisfy a specular reflection condition. This requires the ionized trail to be tangential to a prolate spheroid whose foci are at the transmitter and receiver terminals (see Fig. 2). The fraction of incident meteor trails which are expected to have usable orientations is approximately 5% in the area of the sky which is most effective. Figure 5 shows the estimated percentages of useful trails for a terminal separation of 1 000 km. It may be seen that the optimum scattering regions are situated about 100 km to either side of the great circle, independent of path length.

The fraction of usable trails, p, for any path length, D', can be estimated using the following formula:

$$p = \frac{4L}{3\pi D'} \frac{\left[3\,(\xi^2 - \eta^2) - (1 - \eta^2)\right]\left[(\xi^2 - 1)\,(\xi^2 - \eta^2) - 4\xi^2\,h^2/D'^2\right] - 4\eta^2\,(\xi^2 - 1)\,h^2/D'^2}{(\xi^2 - \eta^2)^2\,(\xi^2 - 1)\left[(\xi^2 - 1)\,(\xi^2 - \eta^2) - 4\xi^2\,h^2/D'^2\right]^{1/2}} \tag{16}$$

where:

$$\xi = (R_1 + R_2)/D'$$

$$\eta = (R_1 - R_2)/D'.$$

8　　Estimating the useful burst rate

An assessment of the link power budget of a meteor-burst communication link can be made using the average trail height and other expressions presented above. Once a link appears viable, a more detailed analysis is required to estimate the rate at which useful meteor-burst signals will be passed.

The most rigorous methods of estimating useful burst rate typically involve the following stages:

a)　establish the minimum useful received signal power;

b)　utilize the equations of § 5 to describe the variation of system parameters;

c)　compute the fraction of useful trails as a function of scattering position using equation (16);

d)　combine the estimated true height distribution of meteor trails with equation (2) to compute the volume density of meteor trails, as a function of q, in the atmosphere;

e)　integrate the product of c) and d) over the meteor region using at each point q_{min} derived at b).

FIGURE 5

**Estimated percentages of useful trails as a function of
scattering position for a terminal separation of 1 000 km**
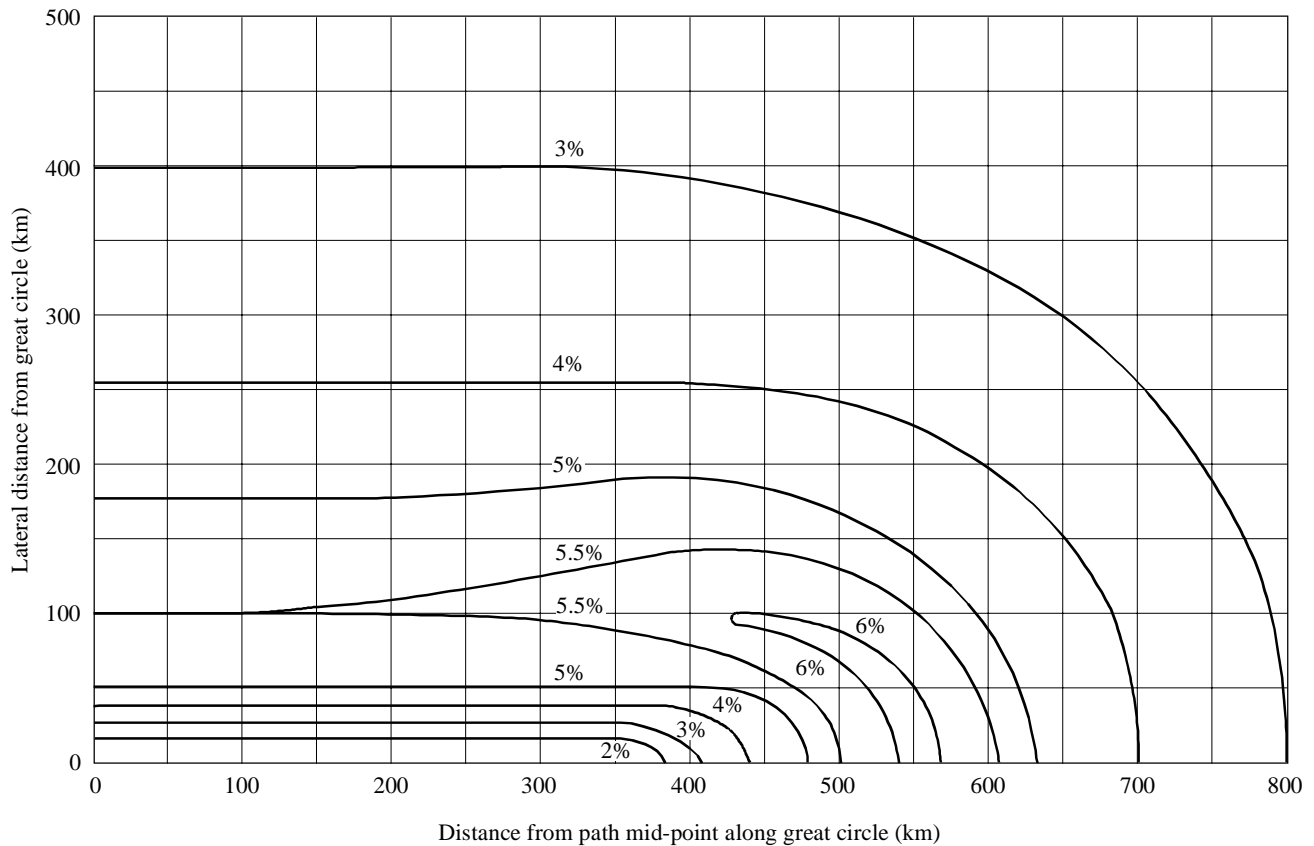
0843-05

9 Antenna considerations

The effect described in § 7, together with the fact that the trails lie mainly in the height range 90-110 km, serve to establish the two "hot-spot" regions towards which both antennas should be directed. The two hot-spots vary in relative importance according to time of day and path orientation. Generally, antennas used in practice should have beams broad enough to cover both hot-spots. Thus the performance is not optimized, but on the other hand the need for beam swinging does not arise.

In general, horizontal polarization is preferred but vertical polarization could be useful for ranges in excess of approximately 1 000 km where low angle cover is required from the antennas.

10 Considerations in the choice of frequency

The choice of frequency in a meteor-burst communication system is influenced by several factors.

10.1 Information duty cycle

The wavelength dependences of the maximum received power, p_{Rmax} and the duty cycle, D_C, as implied by equation (5) are such that for fixed transmitter power and antenna gains:

$$p_{R_{max}} \sim \lambda^3 \qquad (17)$$

This relationship holds for both underdense and overdense trails. The effect on the duty cycle will depend on the relative occurrence rate of these two types of trail. Assuming an intermediate occurrence rate, the duty cycle varies with wavelength as follows:

$$D_C \sim p_{R_{max}} \, T_{un} \tag{18}$$

$$\sim \lambda^5$$

In very quiet receiving locations the predominant noise at frequencies above 25 MHz is cosmic noise and the intensity of this varies as $\lambda^{2.3}$. Hence the information duty cycle, I_C, for a given bandwidth, i.e. the proportion of time a given signal/noise ratio is exceeded, varies with wavelength as follows:

$$I_C \sim \lambda^{2.7} \tag{19}$$

The relative frequency of occurrence of reflections as a function of signal amplitude depends on the sensitivity of the system. A common experimental result in the systems used so far may be expressed as:

$$D_C \sim p_R^{-0.6} \tag{20}$$

where:

D_C: duty cycle (proportion of time exceeding the threshold A)

p_R: received power corresponding to the threshold A.

Since noise power is proportional to bandwidth B, the use of equation (20) leads to:

$$I_C \sim B^{-0.6} \tag{21}$$

The average channel capacity, C, is the product of the signalling rate and the information duty cycle. The former term may be assumed to be proportional to the bandwidth. Therefore the average channel capacity is related to the bandwidth as follows:

$$C \sim B^{0.4} \tag{22}$$

For maximum information transfer the bandwidth should be as large as possible.

Apart from questions of bandwidth availability, the increased noise in a wider bandwidth and hence the decreased availability of the required signal/noise ratio, leads to a reduction in the information duty cycle; this in turn implies longer message delays. Moreover, a point is reached where the system has to rely on overdense trails in which case equation (20) no longer holds. When the exponent of p_R to which D_C is proportional becomes less than –1 there is no advantage in speeding up the rate of signalling. It may be noted that the exponent is liable to fall below –1 for frequencies below 40 MHz on account of ionospheric scatter signals masking the weaker meteor-burst signals.

The usable bandwidth is not likely to be limited by the coherence bandwidth, since this is of the order of several megahertz for the main part of the burst. Even during the tails of the bursts, where there is fading on account of wind shears, the coherence bandwidth is some hundreds of kilohertz.

10.2   Interference

The high path loss associated with meteor-burst communication signals requires that the level of interfering signals be kept to a minimum. As a consequence, the operating frequency should be above that at which normal ionospheric modes propagate.

10.3   Ionospheric absorption

Ionospheric absorption should be minimized which requires the use of as high a frequency as possible. This is particularly of concern for systems operated at high latitudes, where auroral and polar cap absorption can attenuate and even totally absorb the signal if the operating frequency is too low.

10.4   Faraday rotation

At certain times Faraday rotation of meteor-burst communication signals will severely reduce the communication link capacity for frequencies below about 40 MHz.

The first influence is in conflict with the latter three, and when making his frequency choice the system designer must judge the appropriate weightings to be assigned to each.
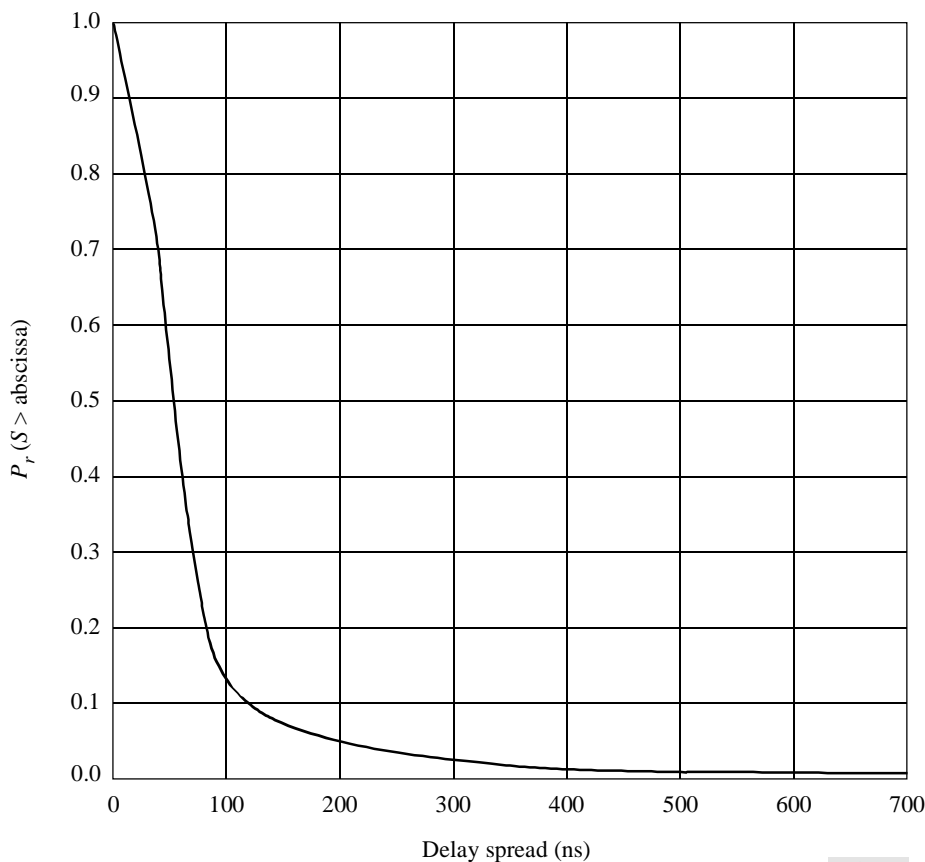
11   Doppler effects

Reflection from the head of a meteor gives rise to Doppler frequency shifts which may span the whole of the audio band. The Doppler frequency shift from a meteor trail is the result of ionospheric wind motions and could be of the order of 20 Hz at a frequency of 40 MHz. Propagation mechanisms, other than meteor scatter, may result in greater multipath and Doppler spreads.

12   Multipath effects

An analysis of impulse response profiles collected on a 500 km meteor-burst link shows that most of the time only a single path exists between the transmitter and receiver, and consequently the signalling rate is unimpeded by the presence of multipath propagation. Only 12% of all underdense trails and 71% of all overdense trails showed any evidence of multipath. This fact is reflected by the delay spread distribution (see Fig. 6) which shows that for 90% of the time the r.m.s. delay spread, S, is less than 100 ns and for 99% of the time the r.m.s. delay spread is less than 400 ns. It should be noted that in several rare instances r.m.s. delay spreads ranging from 1.0 to 7.0 µs have been reported. In the light of this evidence, it can be concluded that trail conditions causing large delay spreads are relatively infrequent.

FIGURE 6

Delay spread statistics

0843-06